VIP Nanocatalysis Very Important Paper

Deutsche Ausgabe: DOI: 10.1002/ange.201600799
Internationale Ausgabe: DOI: 10.1002/anie.201600799

A Tandem Catalyst with Multiple Metal Oxide Interfaces Produced by Atomic Layer Deposition

Huibin Ge, Bin Zhang, Xiaomin Gu, Haojie Liang, Huimin Yang, Zhe Gao, Jianguo Wang, and Yong Qin**

Abstract: *Ideal heterogeneous tandem catalysts necessitate the rational design and integration of collaborative active sites. Herein, we report on the synthesis of a new tandem catalyst with multiple metal-oxide interfaces based on a tube-in-tube nanostructure using template-assisted atomic layer deposition, in which Ni nanoparticles are supported on the outer surface of the inner Al_2O_3 nanotube (Ni/Al_2O_3 interface) and Pt nanoparticles are attached to the inner surface of the outer TiO_2 nanotube (Pt/TiO_2 interface). The tandem catalyst shows remarkably high catalytic efficiency in nitrobenzene hydrogenation over Pt/TiO_2 interface with hydrogen formed in situ by the decomposition of hydrazine hydrate over Ni/Al_2O_3 interface. This can be ascribed to the synergy effect of the two interfaces and the confined nanospace favoring the instant transfer of intermediates. The tube-in-tube tandem catalyst with multiple metal-oxide interfaces represents a new concept for the design of highly efficient and multifunctional nanocatalysts.*

Tandem catalysis has attracted increasing attention, because it can combine multiple chemical transformations in one synthetic operation without separation, purification and transfer of intermediates in each step, thereby saving cost and reducing waste.[1] A series of one-pot tandem catalysis processes have been proposed, but most of these processes employ homogeneous catalysts, resulting in difficulty in product separation and catalyst recyclability.[2] Many efforts have been devoted to the design of heterogeneous tandem catalysts, in which different active sites catalyzing different reactions are immobilized on a support.[1b,3] Metal nanoparticles supported on oxides are widely used in heterogeneous catalysis.[4] The catalytic performance of the metal nanoparticle can be modulated by changing its constitution, shape, size, crystal surfaces, metal-oxide interface, and so on.[1b,5] The integration of different metal-oxide interfaces can yield new tandem catalysts for multistep reactions. However, it is difficult to control the composition and microstructure of multiple metal-oxide interfaces in atomic level by traditional methods.[6]

Atomic layer deposition (ALD) is a high-level film deposition technology by which metals, oxides, polymers, and other materials are deposited on the surface of substrates via sequential self-limiting reactions.[7] It has outstanding advantages in synthesis of uniform nanoparticles and thin films with precise size and film thickness control.[6] A series of advanced catalysts have been synthesized by ALD.[8] ALD was also employed to engineer the metal-oxide interface by coating the surface of metal nanoparticles with ultra-thin oxide films.[5d,8a,b] Recently, we have introduced a general template approach assisted by ALD to fabricate a multiply confined Ni-based catalyst with greatly enhanced activity and stability by optimizing metal-oxide interface.[9]

Herein, we report on a facile template-assisted method based on ALD to synthesize a new tandem catalyst with multiple metal-oxide interfaces (note that the active sites also possibly exist on the surface of metal nanoparticle besides the interface even if the effect of the interface is emphasized in this work). It was previously reported that Ni/Al_2O_3 catalyst can catalyze the decomposition of hydrazine hydrate ($N_2H_4{\cdot}H_2O$) to give hydrogen with high selectivity and efficiency,[10] and that Pt/TiO_2 catalyst can catalyze nitrobenzene hydrogenation at room temperature.[11] Therefore, in this work, we assembled the Ni/Al_2O_3 and Pt/TiO_2 interfaces in a tube-in-tube nanostructure by ALD using carbon nanocoils (CNCs) as templates, thus Ni nanoparticles are supported on the outer surface of the inner Al_2O_3 nanotubes (Ni/Al_2O_3 interface) and Pt nanoparticles are attached to the inner surface of the outer TiO_2 nanotubes (Pt/TiO_2 interface). This tandem catalyst shows remarkably high catalytic efficiency in nitrobenzene hydrogenation with hydrogen formed in situ by the decomposition of $N_2H_4{\cdot}H_2O$.

Figure 1 shows our strategy to prepare the tandem catalyst with two distinct metal-oxide interfaces by ALD. First, an Al_2O_3 layer (150 cycles) is deposited on the surface of CNCs, which have a lower annealing temperature for convenient removal than carbon nanotubes.[12] Second, NiO nanoparticles (200 cycles) are deposited onto the surface of Al_2O_3 layer to form NiO/Al_2O_3 interface. Third, the NiO/Al_2O_3 interface is coated with polyimide (PI) film (100 cycles) to form a sacrificial layer. Fourth, Pt nanoparticles (10 cycles) are deposited on the PI film. Finally, a TiO_2 layer (300 cycles) is deposited to form the Pt/TiO_2 interface. The Al/Ni-Pt/Ti tandem catalyst with Ni/Al_2O_3 and Pt/TiO_2 interfaces is obtained after O_2 calcination to remove the template and sacrificial layer and H_2/Ar reduction. This method can realize conveniently assembling of suitable metal-oxide interfaces for

[*] H. B. Ge, Dr. B. Zhang, X. M. Gu, H. J. Liang, H. M. Yang, Dr. Z. Gao, Prof. J. G. Wang, Prof. Y. Qin
State Key Laboratory of Coal Conversion
Institute of Coal Chemistry, Chinese Academy of Sciences
27 Taoyuan South Road, Taiyuan 030001 (P.R. China)
E-mail: zhangbin2009@sxicc.ac.cn
qinyong@sxicc.ac.cn
H. B. Ge, X. M. Gu, H. J. Liang
University of Chinese Academy of Sciences
Beijing, 100049 (P.R. China)

Supporting information for this article can be found under: http://dx.doi.org/10.1002/anie.201600799.

 © 2016 Wiley-VCH Verlag GmbH & Co. KGaA, Weinheim

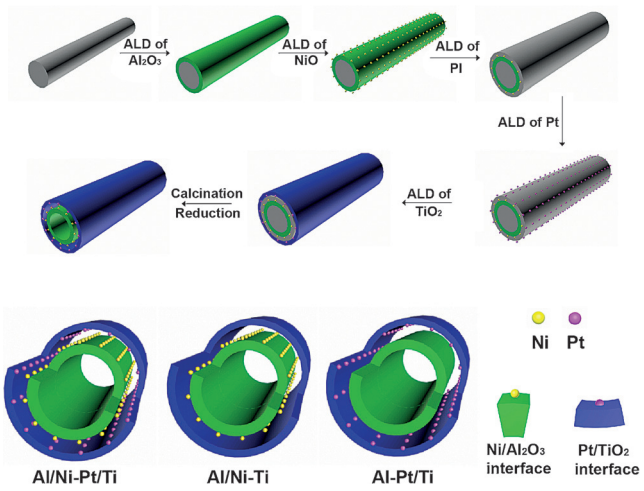

Figure 1. Schematic illustration of the procedure for the synthesis of the tandem catalyst with both Ni/Al_2O_3 and Pt/TiO_2 interfaces and semi-sectional views of different catalysts for comparison.

a given tandem reaction. For comparison, the catalysts with one metal-oxide interface, labeled as Al-Pt/Ti and Al/Ni-Ti, were also prepared by the same method but without deposition of NiO or Pt during the ALD sequences, respectively.

Figure 2A (also Figure S1) shows the transmission electron microscopy (TEM) image of the Al/Ni-Pt/Ti catalyst. We can clearly observe the void space between the inner Al_2O_3 nanotube and outer TiO_2 nanotube of the tube-in-tube nanostructure. The void space between the two shells is approximately 10 nm in thickness, which is consistent with the thickness of polyimide film. The wall thicknesses of Al_2O_3 nanotubes and TiO_2 nanotubes are about 15 nm and 12 nm, respectively. The Ni nanoparticles with a diameter of 6.3 ± 1.3 nm are dispersed homogeneously on the outer surface of Al_2O_3 nanotube, while Pt nanoparticles (less than 1 nm) confined in TiO_2 nanotube are too small to be observed.[5c] Figure 2B and 2C show that both Al/Ni-Ti and Al-Pt/Ti catalysts have a similar tube-in-tube structure as the Al/Ni-Pt/Ti catalyst. The Al/Ni-Ti catalyst shows a similar size distribution of Ni nanoparticles as the Al/Ni-Pt/Ti catalyst. High-angle annular dark field scanning transmission electron microcopy (HAADF-STEM) and energy-dispersive X-Ray spectrometry (EDX) analysis (Figure 2D and 2E) were used to reveal the element distribution in the microstructure of the Al/Ni-Pt/Ti catalyst. The HAADF-STEM image of the Al/Ni-Pt/Ti catalyst provides a clear contrast for the inner Al_2O_3 nanotube, the Ni nanoparticles supported on the surface of Al_2O_3 nanotube, the void space, and the TiO_2 nanotube. EDX element mapping (Figure 2E) clearly reveals the existence of Al, Ni, Pt, and Ti. Their distribution is consistent with the positions of Al_2O_3, Ni, Pt and TiO_2 layers. In particular, the Pt element is exactly detected although it is not clearly visible by TEM investigation due to small size and the thick TiO_2 shells. Inductively coupled plasma optical emission spectrometry (ICP-OES) analysis shows that the Pt content is about 0.43 wt% for Al/Ni-Pt/Ti and Al-Pt/Ti, and the Ni content is about 2.5 wt% for Al/Ni-Pt/Ti and Al/Ni-Ti (see Table S1 in the Supporting Information).

Extended X-ray absorption fine structure (EXFAS) spectra were measured on fresh reduced catalysts. Figure 3A shows the normalized X-ray adsorption near-edge structure (XANES) of fresh reduced Al/Ni-Pt/Ti and Al-Pt/Ti catalysts. The white line intensities of both catalysts are similar to that of Pt foil, indicating the dominance of Pt^0 nanoparticles in Al/Ni-Pt/Ti and Al-Pt/Ti catalysts. In the Fourier transforms (*r* space, Figure 3B) of EXAFS data, the peaks at 1.0–2.0 Å in the PtO_2 are due to scattering from the nearest O, while the peaks at 2.0–3.3 Å in the Pt foil are due to scattering from the

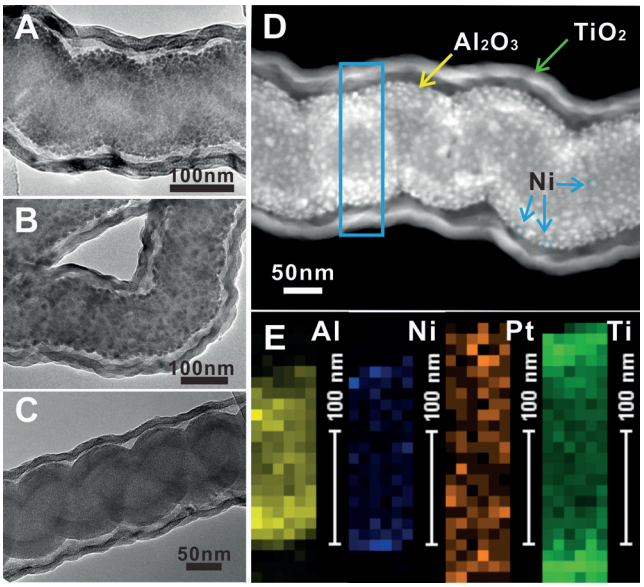

Figure 2. TEM images of the catalyst Al/Ni-Pt/Ti (A), Al/Ni-Ti (B) and Al-Pt/Ti (C). D) HAADF-STEM image of Al/Ni-Pt/Ti. E) EDX elemental mapping of Al/Ni-Pt/Ti for the boxed area in (D).

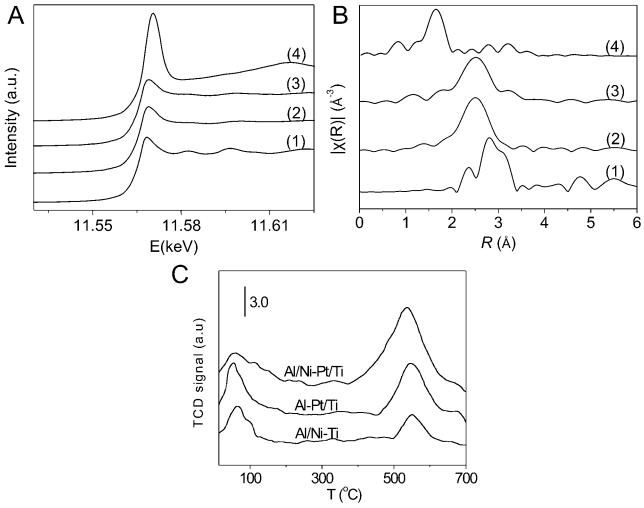

Figure 3. A) The normalized intensity of Pt L_3-XANES spectra. B) Corresponding Fourier transform k^3-weighted EXAFS spectra (without phase correction): (1) Pt foil; (2) Al/Ni-Pt/Ti; (3) Al-Pt/Ti; (4) PtO_2. $\Delta k = 2.8–10.8$ Å^{-1} was used for Al/Ni-Pt/Ti and Al-Pt/Ti; $\Delta k = 2.8–13.3$ Å^{-1} was used for Pt foil and PtO_2. C) H_2-TPD profiles of Al/Ni-Pt/Ti, Al/Ni-Ti, and Al-Pt/Ti.

© 2016 Wiley-VCH Verlag GmbH & Co. KGaA, Weinheim

neighboring Pt. Both Al/Ni-Pt/Ti and Al-Pt/Ti samples have one prominent peak at 2.5 Å from either Pt-Ti or Pt-Pt contributions. The weak peaks at 1.2 and 1.7 Å can be assigned to the Pt-O contribution, while the weak peak at 3.2 Å can be assigned to the Pt-Pt contribution. Therefore, the Pt/TiO_2 interface on Al/Ni-Pt/Ti and Al-Pt/Ti is similar.

The Al/Ni-Pt/Ti catalyst with two different metal-oxide interfaces is an ideal catalyst for the tandem hydrogenation of nitrobenzene to aniline using $N_2H_4{\cdot}H_2O$ as hydrogen source as a probe reaction. Figure 4A (also Figure S2 and Table S1) shows that the catalytic activity of the Al/Ni-Pt/Ti catalyst is significantly higher than that of the Al/Ni-Ti and Al-Pt/Ti catalysts with a single metal-oxide interface. Almost no reaction occurs over the Al-Pt/Ti catalyst, and little aniline is obtained over Al/Ni-Ti catalyst. The evolution of nitrobenzene conversion over Al/Ni-Pt/Ti catalyst with the reaction time at 40 °C was investigated (Figure S3). As we expected, the reaction can be efficiently catalyzed by the Al/Ni-Pt/Ti catalyst with high activity and high selectivity of aniline (ca. 99 %). The Al/Ni-Pt/Ti catalyst was reused for four consecutive cycles and only slight reduction in catalytic activity was observed, revealing good stability (Figure S4).

Previous reports show that Ni/Al_2O_3 catalysts have a high catalytic performance in decomposition of $N_2H_4{\cdot}H_2O$ to H_2 and N_2.[10] Control experiments were performed for the decomposition of $N_2H_4{\cdot}H_2O$ at 40 °C. Figure 4B shows that the H_2-generation rate from $N_2H_4{\cdot}H_2O$ decomposition over the Al/Ni-Ti catalyst is 18 mmol g_{cat}^{-1} h^{-1}, which is similar to that of the Al/Ni-Pt/Ti catalyst (22 mmol g_{cat}^{-1} h^{-1}). This reveals that the decomposition of $N_2H_4{\cdot}H_2O$ only occurs on the Ni/Al_2O_3 interface, since the Al-Pt/Ti catalyst has no catalytic activity in $N_2H_4{\cdot}H_2O$ decomposition.

Figure 4C shows the reaction rate of different catalysts for nitrobenzene hydrogenation in 20 bar H_2. The Al/Ni-Ti catalyst has a rather low catalytic activity (2 mmol g_{cat}^{-1} h^{-1}), while the reaction rate is 32 mmol g_{cat}^{-1} h^{-1} over the Al/Ni-Pt/Ti catalyst and 9 mmol g_{cat}^{-1} h^{-1} over the Al-Pt/Ti catalyst, confirming that the nitrobenzene hydrogenation is catalyzed by the Pt/TiO_2 interface. The reaction rate over the Al/Ni-Pt/Ti catalyst is higher than that over the Al-Pt/Ti catalyst. H_2-chemsorption analysis (Table S1) shows that the H_2 uptake on Al/Ni-Pt/Ti (19.2 μmol g^{-1}) is close to the sum of that on Al/Ni-Ti (5.9 μmol g^{-1}) and Al-Pt/Ti (12.1 μmol g^{-1}). Therefore, the increase of reaction rate is not due to the increase of active sites but the synergy of two interfaces in the Al/Ni-Pt/Ti catalyst. In addition, it is found that the activity increases with the increase of hydrogen pressure for the Al/Ni-Pt/Ti catalyst (Figure S5). The reaction order of H_2 for selective nitrobenzene hydrogenation was calculated giving a value of about 1.1 over the Al/Ni-Pt/Ti catalyst, which suggests that the dissociated adsorption of H_2 is not the rate-determining step and a high concentration of hydrogen favors the hydrogenation. However, the catalytic activity is still much lower than that of the tandem reaction even if the H_2 pressure increases to 20 bar. This demonstrates the advantages of this tandem reaction over direct hydrogenation in terms of the mild conditions.

The combination of collaborative metal-oxide active sites for each step of tandem reaction is absolutely necessary for a high efficiency tandem catalyst. Using ALD, we can easily control the composition and microstructure of multiple metal-oxide interfaces. Therefore, the combination of metal-oxide active sites can be modified by change ALD process. For example, the Pt/TiO_2

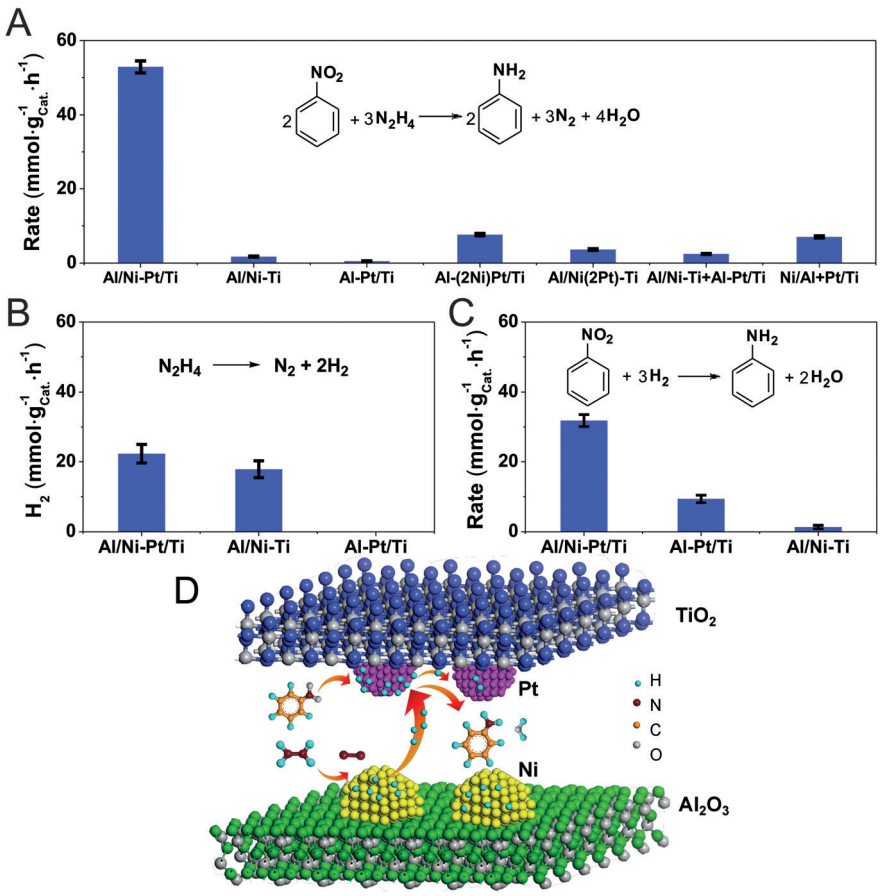

Figure 4. The catalytic performance of different catalysts. A) Activity for nitrobenzene hydrogenation using $N_2H_4{\cdot}H_2O$ as hydrogen source (Reaction conditions: 50 μL nitrobenzene, 200 μL hydrazine hydrate, 10 mL water–ethanol mixture (v/v = 1/1), and 10 mg catalyst at 40 °C; Physical mixture catalysts of Al/Ni-Ti + Al-Pt/Ti containing 10 mg Al/Ni-Ti and 10 mg Al-Pt/Ti; Physical mixture catalysts of Ni/Al + Pt/Ti containing 5 mg Ni/Al_2O_3 and 5 mg Pt/TiO_2). B) Activity for H_2 generation from $N_2H_4{\cdot}H_2O$ decomposition (Reaction conditions: 200 μL hydrazine hydrate, 10 mL water, and 10 mg catalyst at 40 °C). C) Activity for hydrogenation of nitrobenzene (Reaction conditions: 50 μL nitrobenzene, 10 mL water–ethanol mixture (v/v = 1/1), and 10 mg catalyst at 40 °C in 20 bar H_2). (D) Illustration of the tandem catalysis on Al/Ni-Pt/Ti catalyst in the aqueous ethanol solution.

© 2016 Wiley-VCH Verlag GmbH & Co. KGaA, Weinheim

interface can be changed to a Pt/Al_2O_3 interface. An Al/Ni-Pt/Al catalyst with Ni/Al_2O_3 and Pt/Al_2O_3 interfaces was prepared by sequential deposition of Al_2O_3 (150 cycles), Ni (200 cycles), PI (100 cycles), Pt (10 cycles), and Al_2O_3 (150 cycles) on CNCs template by ALD, followed by O_2 calcination and H_2/Ar reduction. However, the reaction rate of the Al/Ni-Pt/Al catalyst is only about 10 percent of the Al/Ni-Pt/Ti catalyst in this tandem reaction (Figure S6), because of the low efficiency of Pt/Al_2O_3 interface in nitrobenzene hydrogenation.[11] Therefore, the synergy of the Ni/Al_2O_3 and Pt/TiO_2 interfaces is essential in this tandem reaction.

We have also prepared the Ni modified Pt/TiO_2 (Al-(*m*Ni)Pt/Ti) and Pt modified Ni/Al_2O_3 (Al/Ni(*n*Pt)-Ti) catalysts by sequential deposition of Al_2O_3 (150 cycles), PI (100 cycles), *m* (*m* = 2, 5, 10) cycles of Ni, Pt (10 cycles), and TiO_2 (300 cycles), and Al_2O_3 (150 cycles), Ni (200 cycles), *n* (*n* = 2, 10) cycles of Pt, PI (100 cycles), and TiO_2 (300 cycles) on CNCs templates, followed by O_2 calcination and H_2/Ar reduction, respectively. Figure 4A (also Figure S7) shows the tandem reaction results of these catalysts. It is clearly observed that the catalytic activity of these Al-(*m*Ni)Pt/Ti and Al/Ni(*n*Pt)-Ti is much lower than that of Al/Ni-Pt/Ti, and the catalytic activity of Al-(*m*Ni)Pt/Ti reduces with the increase of Ni deposition cycle numbers from 2 to 10. Therefore, the high catalytic activity of Al/Ni-Pt/Ti is due to the synergy effect of two different metal-oxide interfaces, instead of the formation of Ni modified Pt/TiO_2 interface, Pt modified Ni/Al_2O_3 interface or Pt-Ni alloy/oxide interface.

Hydrogen temperature programmed desorption (H_2-TPD) was conducted for Al/Ni-Pt/Ti, Al/Ni-Ti, and Al-Pt/Ti catalysts (Figure 3C). The high temperature desorption peak (maxima around 540 °C) is generally assigned to spillover hydrogen.[13] The spillover hydrogen on Al/Ni-Pt/Ti (240.6 $\mu mol\,g^{-1}$) is almost 1.5 times more than the sum of that on Al-Pt/Ti (121.0 $\mu mol\,g^{-1}$) and Al/Ni-Ti (45.1 $\mu mol\,g^{-1}$), suggesting the transfer of active hydrogen between two interfaces in the Al/Ni-Pt/Ti catalyst. The transfer of active hydrogen can explain the synergy of two interfaces in the Al/Ni-Pt/Ti catalyst during nitrobenzene hydrogenation (Figure 4C). Generally, H_2 molecule can be activated on acitve transition metal sites, and then spills over to the nearby less active metal sites, and the spillover is reversible.[14] The H_2 dissociation on Pt surface is easier than that on Ni surface.[15] In H_2 atmosphere, the active hydrogen generated from the Pt/TiO_2 interface can spill over to the Ni/Al_2O_3 interface, and results in the increase of reaction rate during nitrobenzene hydrogenation over the Al/Ni-Pt/Ti catalyst.

To further demonstrate the unique properties of the tandem catalyst, the tandem reaction of nitrobenzene hydrogenation using $N_2H_4{\cdot}H_2O$ as hydrogen source was examined over physical mixture of Al/Ni-Ti and Al-Pt/Ti catalysts (Al/Ni-Ti + Al-Pt/Ti), and physical mixture of Ni/Al_2O_3 and Pt/TiO_2 catalysts (Ni/Al + Pt/Ti) (Figure 4A). The Ni/Al_2O_3 catalyst and Pt/TiO_2 catalyst were prepared by sequential deposition of Al_2O_3 (150 cycles) and Ni (200 cycles), or TiO_2 (300 cycles) and Pt (10 cycles) on CNCs template by ALD, followed by O_2 calcination and H_2/Ar reduction, respectively. The catalytic activity of mixed Ni/Al + Pt/Ti catalysts (7 $mmol\,g_{cat}^{-1}\,h^{-1}$) is higher than that of mixed Al/Ni-Ti + Al-Pt/Ti catalysts (2 $mmol\,g_{cat}^{-1}\,h^{-1}$), but still much slower than that of the Al/Ni-Pt/Ti catalyst (53 $mmol\,g_{cat}^{-1}\,h^{-1}$). H_2-chemsorption results show that the number of metal sites on Al/Ni-Pt/Ti is close to the sum of those on Al/Ni-Ti and Al-Pt/Ti. Therefore, the special tube-in-tube geometry of the Al/Ni-Pt/Ti catalyst is crucial to its high catalytic performance, not just the presence of the two types of catalytic sites. Furthermore, the calculated H_2 consumption (159 $mmol\,g_{cat}^{-1}\,h^{-1}$, Figure 4A) during tandem reaction is obviously higher than the H_2 (gas) generation rate (22 $mmol\,g_{cat}^{-1}\,h^{-1}$, Figure 4B) from hydrazine decomposition over the Al/Ni-Pt/Ti catalyst, suggesting that the H_2(gas) pressure in the nanotubes cannot increase during tandem reaction and the rate of $N_2H_4{\cdot}H_2O$ decomposition is accelerated. The $N_2H_4{\cdot}H_2O$ decomposition to H_2 (gas) includes two steps over Ni/Al_2O_3 interface: the decomposition of $N_2H_4{\cdot}H_2O$ to active hydrogen, and the formation and desorption of H_2 (gas)[16] Considering that the $N_2H_4{\cdot}H_2O$ is excess during reaction, the rate of $N_2H_4{\cdot}H_2O$ decomposition depends on the available active sites on Ni/Al_2O_3 interface. Control experiments reveal that a high hydrogen pressure (or high hydrogen coverage) has a negative effect in $N_2H_4{\cdot}H_2O$ decomposition over the Ni/Al_2O_3 catalyst (Figure S12). In the tandem reaction over the Al/Ni-Pt/Ti catalyst, the instant transfer of active hydrogen from $N_2H_4{\cdot}H_2O$ decomposition over Ni/Al_2O_3 interface to Pt/TiO_2 interface for hydrogenation in the confined nanospace results in a lower coverage of active hydrogen on the Ni/Al_2O_3 interface, namely, more available active sites, and therefore accelerates the $N_2H_4{\cdot}H_2O$ decomposition. The low activity for the physical mixture of Al/Ni-Ti and Al-Pt/Ti catalysts is due to the blocking of transfer of active hydrogen by the oxide shell, and the little increase of reaction rate over the mixed Ni/Al + Pt/Ti catalysts may be due to the slight random intermediate transfer between the two catalysts. On the base of above analysis, the high efficiency of the tandem catalyst can be attributed to two reasons. First, the confined nanospace facilitates the instant transfer of the active hydrogen. Second, the synergy effect of the two metal-oxide interfaces enhances the tandem reaction.

In summary, this work has demonstrated a general route to synthesize tandem catalysts with multiple metal-oxide interfaces by ALD. Dramatic activity enhancement has been observed for the tandem catalyst in nitrobenzene hydrogenation with hydrogen formed in situ by $N_2H_4{\cdot}H_2O$ decomposition due to the synergy of Ni/Al_2O_3 and Pt/TiO_2 interfaces in a confined nanospace. The confined nanospace favors the instant transfer of intermediates between the two metal-oxide interfaces. The tube-in-tube tandem catalyst with multiple metal-oxide interfaces represents a new concept for the design of highly efficient and multifunctional nanocatalysts.

Acknowledgements

We appreciate the financial support from the National Natural Science Foundation of China (grant numbers 21403271, 21173248, and 21403272), the Hundred Talents Program of the Chinese Academy of Sciences, the Hundred Talents Program of Shanxi Province, and the Natural Science

 © 2016 Wiley-VCH Verlag GmbH & Co. KGaA, Weinheim

Foundation of Shanxi Province (grant numbers 201411012-1 and 2015021046). EXAFS studies were carried out at BL14W1 beamline at the Shanghai Synchrotron Radiation Facility, Shanghai Institute of Applied Physics, China (15ssrf01920). We thank Prof. Rui Si (Shanghai Institute of Applied Physics, Chinese Academy of Sciences), Pei Sheng, and Guofu Wang (Institute of Coal Chemistry, Chinese Academy of Sciences) for EXAFS characterization.

Keywords: atomic layer depositon · heterogeneous catalysis · hydrogenation · metal-oxide interfaces · nanocatalysis

How to cite: *Angew. Chem. Int. Ed.* **2016**, *55*, 7081 – 7085
Angew. Chem. **2016**, *128*, 7197 – 7201

[1] a) Y. Shiraishi, M. Ikeda, D. Tsukamoto, S. Tanaka, T. Hirai, *Chem. Commun.* **2011**, *47*, 4811 – 4813; b) Y. Yamada, C.-K. Tsung, W. Huang, Z. Huo, S. E. Habas, T. Soejima, C. E. Aliaga, G. A. Somorjai, P. Yang, *Nat. Chem.* **2011**, *3*, 372 – 376; c) T. L. Lohr, T. J. Marks, *Nat. Chem.* **2015**, *7*, 477 – 482.

[2] a) C. Gunanathan, Y. Ben-David, D. Milstein, *Science* **2007**, *317*, 790 – 792; b) J.-C. Wasilke, S. J. Obrey, R. T. Baker, G. C. Bazan, *Chem. Rev.* **2005**, *105*, 1001 – 1020.

[3] a) F.-X. Felpin, E. Fouquet, *ChemSusChem* **2008**, *1*, 718 – 724; b) Y. Shiraishi, Y. Sugano, S. Tanaka, T. Hirai, *Angew. Chem. Int. Ed.* **2010**, *49*, 1656 – 1660; *Angew. Chem.* **2010**, *122*, 1700 – 1704; c) Y. Yang, X. Liu, X. Li, J. Zhao, S. Bai, J. Liu, Q. Yang, *Angew. Chem. Int. Ed.* **2012**, *51*, 9164 – 9168; *Angew. Chem.* **2012**, *124*, 9298 – 9302.

[4] R. J. White, R. Luque, V. L. Budarin, J. H. Clark, D. J. Macquarrie, *Chem. Soc. Rev.* **2009**, *38*, 481 – 494.

[5] a) K. Qadir, S. H. Kim, S. M. Kim, H. Ha, J. Y. Park, *J. Phys. Chem. C* **2012**, *116*, 24054 – 24059; b) F. Zaera, *Chem. Soc. Rev.* **2013**, *42*, 2746 – 2762; c) J. Li, B. Zhang, Y. Chen, J. Zhang, H. Yang, J. Zhang, X. Lu, G. Li, Y. Qin, *Catal. Sci. Technol.* **2015**, *5*, 4218 – 4223; d) B. Zhang, Y. Chen, J. Li, E. Pippel, H. Yang, Z. Gao, Y. Qin, *ACS Catal.* **2015**, *5*, 5567 – 5573.

[6] B. J. O'Neill, D. H. K. Jackson, J. Lee, C. Canlas, P. C. Stair, C. L. Marshall, J. W. Elam, T. F. Kuech, J. A. Dumesic, G. W. Huber, *ACS Catal.* **2015**, *5*, 1804 – 1825.

[7] a) S. M. George, *Chem. Rev.* **2010**, *110*, 111 – 131; b) J. L. Lu, J. W. Elam, P. C. Stair, *Acc. Chem. Res.* **2013**, *46*, 1806 – 1815.

[8] a) J. Lu, B. Fu, M. C. Kung, G. Xiao, J. W. Elam, H. H. Kung, P. C. Stair, *Science* **2012**, *335*, 1205 – 1208; b) B. J. O'Neill, D. H. K. Jackson, A. J. Crisci, C. A. Farberow, F. Shi, A. C. Alba-Rubio, J. Lu, P. J. Dietrich, X. Gu, C. L. Marshall, P. C. Stair, J. W. Elam, J. T. Miller, F. H. Ribeiro, P. M. Voyles, J. Greeley, M. Mavrikakis, S. L. Scott, T. F. Kuech, J. A. Dumesic, *Angew. Chem. Int. Ed.* **2013**, *52*, 13808 – 13812; *Angew. Chem.* **2013**, *125*, 14053 – 14057; c) J. Lu, K.-B. Low, Y. Lei, J. A. Libera, A. Nicholls, P. C. Stair, J. W. Elam, *Nat. Commun.* **2014**, *5*, 3264; d) H. Yan, H. Cheng, H. Yi, Y. Lin, T. Yao, C. Wang, J. Li, S. Wei, J. Lu, *J. Am. Chem. Soc.* **2015**, *137*, 10484 – 10487.

[9] Z. Gao, M. Dong, G. Wang, P. Sheng, Z. Wu, H. Yang, B. Zhang, G. Wang, J. Wang, Y. Qin, *Angew. Chem. Int. Ed.* **2015**, *54*, 9006 – 9010; *Angew. Chem.* **2015**, *127*, 9134 – 9138.

[10] L. He, Y. Huang, A. Wang, X. Wang, X. Chen, J. J. Delgado, T. Zhang, *Angew. Chem. Int. Ed.* **2012**, *51*, 6191 – 6194; *Angew. Chem.* **2012**, *124*, 6295 – 6298.

[11] A. Corma, P. Serna, P. Concepción, J. J. Calvino, *J. Am. Chem. Soc.* **2008**, *130*, 8748 – 8753.

[12] Y. Qin, Z. Zhang, Z. Cui, *Carbon* **2004**, *42*, 1917 – 1922.

[13] R. Kramer, M. Andre, *J. Catal.* **1979**, *58*, 287 – 295.

[14] a) W. C. Conner, J. L. Falconer, *Chem. Rev.* **1995**, *95*, 759 – 788; b) G. Kyriakou, M. B. Boucher, A. D. Jewell, E. A. Lewis, T. J. Lawton, A. E. Baber, H. L. Tierney, M. Flytzani-Stephanopoulos, E. C. H. Sykes, *Science* **2012**, *335*, 1209 – 1212; c) M. D. Marcinkowski, A. D. Jewell, M. Stamatakis, M. B. Boucher, E. A. Lewis, C. J. Murphy, G. Kyriakou, E. C. H. Sykes, *Nat. Mater.* **2013**, *12*, 523 – 528.

[15] J. Wu, S. W. Ong, H. C. Kang, E. S. Tok, *J. Phys. Chem. C* **2010**, *114*, 21252 – 21261.

[16] a) H. L. McKay, S. J. Jenkins, D. J. Wales, *J. Phys. Chem. C* **2011**, *115*, 17812 – 17828; b) P.-X. Zhang, Y.-G. Wang, Y.-Q. Huang, T. Zhang, G.-S. Wu, J. Li, *Catal. Today* **2011**, *165*, 80 – 88; c) S. S. Tafreshi, A. Roldan, N. H. de Leeuw, *Phys. Chem. Chem. Phys.* **2015**, *17*, 21533 – 21546.

Received: January 24, 2016
Published online: April 28, 2016

 © 2016 Wiley-VCH Verlag GmbH & Co. KGaA, Weinheim